Tensile Pulse Generation Techniques in a Split Hopkinson Bar

J. F. Acosta* and K. S. Raju

Department of Aerospace Engineering, College of Engineering

Abstract. Experimental testing in a tensile Split Hopkinson Pressure Bar showed that the generated tensile pulse using a transfer flange methodology differs from the theoretical prediction. Flange attachment technique to incident bar and flange dimensions distort pulse shape and alter pulse width. Secondary pulses are introduced that hinder the calibration of the testing apparatus and its application to recovery experiments to study history effects. Lagrange diagrams are used to visualize pulse propagation and to identify secondary pulses sources. Geometrical parameters that hinder a proper generation and transfer of the loading pulse are identified and the effect on pulse characteristics is quantified using an Ls-Dyna explicit finite element model.

1. Introduction

The Split Hopkinson Pressure Bar (SHPB) for tensile impact testing follows the same principles and data analysis as the classical SHPB. However, tensile and compression systems differ on the technique to grip the specimen, the methodology for introducing a tensile loading pulse, and the testing specimen geometry. The main criterion for selecting a load transfer methodology, such that it allows for a proper calibration of the testing apparatus, is the reliability of the generated tensile pulse. In the present investigation, direct tensile loading is generated after impacting a flange attached on the end of the incident bar with a hollow striker bar, see Figure 1. From the impact, a tensile pulse is generated on the incident bar and propagated down to a specimen. At the interface, the pulse is partially transmitted through the specimen onto the transmitted bar as a tensile pulse and partially reflected back into the incident bar as a compressive pulse [1]. The aspect ratio between the dimensions of the flange and the striker would shape the resulting pulse. Wave propagation is evaluated through every component on the apparatus, and the pulse's superposition is detected and corrected.

2. Experiment, Results, Discussion, and Significance

There are a few possibilities to attach the flange to the bar, i.e., clamp, threaded, welded, or a press fitted connection. As an alternative option a sleeve flange is proposed. It is clamped to the end of the incident bar over a matching profile. The sleeve is compounded of two halves that are fastened together (see Figure 2). Other types of connections may observe stress concentration at the bar-flange interface, i.e., fatigue can degrade the connection.

Experimental tests were conducted on a Tensile SHPB. Strain history for two flange locations are presented in Figure 3. Pulses observe large oscillations after the initial peak. Secondary pulses, result of subsequent reflections, are over imposed to transverse oscillations result of Poisson effect. Pulse superposition is visualized in the Lagrange diagram in Figure 4. The tensile pulse, and its symmetric compressive pulse, can be traced as they travel and reach each interface. Strain history is plotted on the right. The leading pulse has not crossed the strain gage entirely when a secondary pulse reaches the gage. Final output is a summation of pulses extending the pulse width and altering pulse shape. Superposition cannot be fixed by simply changing the location of the gages. A pulse under these conditions cannot be use for strain rate studies, system calibration, or history effects studies.

An explicit finite element model was created for the simulation using the commercial code Ls-Dyna. In the simulation a hollow cylindrical striker of length Ls is fired against a transfer flange of length Lf with a velocity 20 m/s. Penalty formulation is used for the contact analysis. Automatic surface to surface contacts were specified at the interfaces between striker, the transfer flange, and the incident bar. Linear elastic isotropic material properties for aluminum 7075-T6 were defined. Element size of 3 mm was used based on mesh sensitivity studies [2].

Numerical and experimental observations suggested the addition of a momentum trap after the transfer flange. It would contain the compressive momentum generated at the collision of the striker and the flange, see Figure 4. Lagrange diagram on Figure 5 shows the compressive pulse being trapped after crossing the flange. After reaching the back face of the trap it reflects as a tensile pulse, but since there is not attachment between the flange and the trap, the tensile pulse gets truncated and simply moves the trap apart from the flange. A momentum trap 254 mm long is included in the simulation of the general type flange and in the simulation of the sleeve flange. General type

flange dimensions are 15.24 mm length and 20.9 mm height. Sleeve flange dimensions are 76.2 mm long and 25.4 mm radius. The effect of the trap on the loading pulse is compared with previous simulations where no momentum trap is included (see Figure 6). Pulse width observed an error of only 15.73 % compared to the theoretical width.

3. Conclusions

Pulse characteristics as width, amplitude, shape, and levels of oscillations were evaluated experimentally using a Tensile SHPB apparatus. Results were compared with analytical models for improvements. Examining such characteristics allowed understanding of the mechanics of the momentum transfer and the tensile load generation on the incident bar. An improvement on the transfer flange technique was achieved by simply adding a momentum trap to the apparatus. This is an alternative that minimizes load levels on the flange-bar intersection since the trap contains the compressive momentum and prevents any additional tensile loading over the incident bar. Results showed a significant improvement reducing the load levels and minimizing the distortion of the pulse. A momentum trap in combination with a sleeve flange not only reduces the load levels on the connection but also provides control over the pulse width. Secondary pulses are restrained and fatigue related problems are lessened.

[1] Li, A. and Lambros, J., "Dynamic Thermomechanical Behavior of Fiber Reinforced Composites," Composites: Part A, Vol. 31, 2000, 537-47.
[2] Govender, R. A., Cloete, T. J., and Nurick, G. N., "A Numerical Investigation of Dispersion in Hopkinson Pressure Bar Experiments," J. Phys. IV France., Vol. 134, 2006, pp. 521-526.

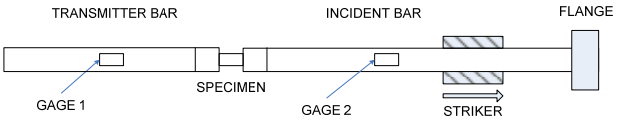

Fig. 1. Flange loading methodology.

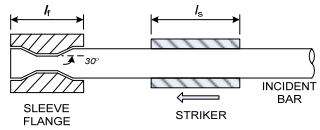

Fig. 2. Sleeve flange at bar end.

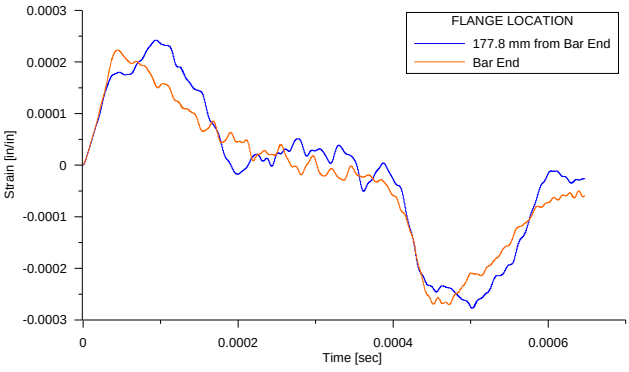

Fig. 3. Strain history on incident bar.

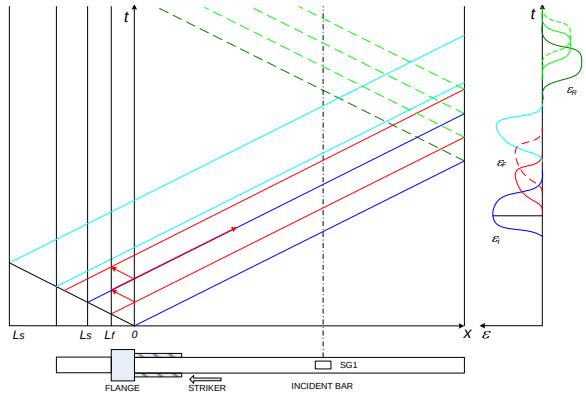

Fig. 4. Lagrange diagram for sleeve flange.

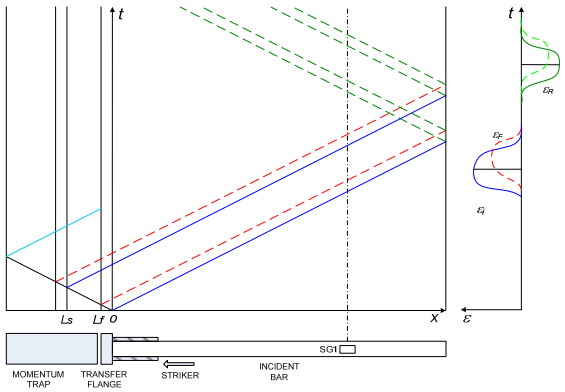

Fig. 5. Lagrange diagram for momentum trap.

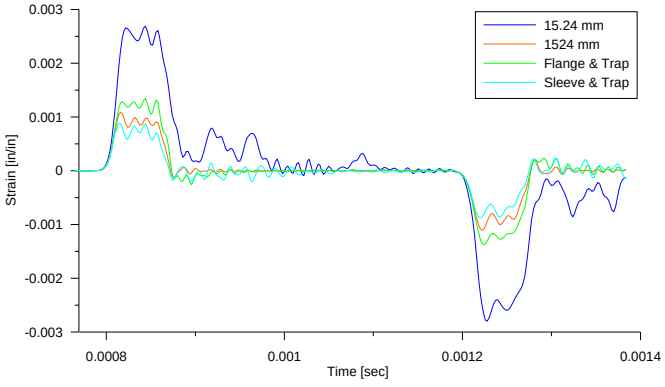

Fig. 6. Strain history comparison.